Bifunctional Nanostructure of Magnetic Core Luminescent Shell and Its Application as Solid-State Electrochemiluminescence Sensor Material

Lihua Zhang, Baifeng Liu, and Shaojun Dong*

State Key Laboratory of Electroanalytical Chemistry, Changchun Institute of Applied Chemistry, Graduate School of the Chinese Academy of Sciences, Chinese Academy of Sciences, Changchun, 130022, China

Received: May 5, 2007; In Final Form: June 29, 2007

Bifunctional nanoarchitecture has been developed by combining the magnetic iron oxide and the luminescent $Ru(bpy)_3^{2+}$ encapsulated in silica. First, the iron oxide nanoparticles were synthesized and coated with silica, which was used to isolate the magnetic nanoparticles from the outer-shell encapsulated $Ru(bpy)_3^{2+}$ to prevent luminescence quenching. Then onto this core an outer shell of silica containing encapsulated $Ru(bpy)_3^{2+}$ was grown through the Stöber method. Highly luminescent $Ru(bpy)_3^{2+}$ serves as a luminescent marker, while magnetic Fe_3O_4 nanoparticles allow external manipulation by a magnetic field. Since $Ru(bpy)_3^{2+}$ is a typical electrochemiluminescence (ECL) reagent and it could still maintain such property when encapsulated in the bifunctional nanoparticle, we explored the feasibility of applying the as-prepared nanostructure to fabricating an ECL sensor; such method is simple and effective. We applied the prepared ECL sensor not only to the typical $Ru(bpy)_3^{2+}$ co-reactant tripropylamine (TPA), but also to the practically important polyamines. Consequently, the ECL sensor shows a wide linear range, high sensitivity, and good stability.

1. Introduction

Nanoparticles have unique, size-dependent properties; therefore, they are of increasing interest for both fundamental research and numerous applications.[1] In addition, magnetic nanoparticles are important materials due to their interesting magnetic properties, and they have been sophisticatedly employed in many advanced technology areas.[2−6] Magnetic adsorbents, carriers, and modifiers can be used for the immobilization, isolation, modification, detection, determination, and removal of a variety of biologically active compounds, xenobiotics, cellular components, and cells. Moreover, magnetic separation and labeling have recently been attracting more attention, particularly in molecular and cell biology, microbiology, biochemistry, and bioanalytical chemistry.[7−10] On the other hand, magneto-controlled molecular electronics and bioelectronics are new topics that examine the effect of an external field on electrochemical and bioelectrochemical processes of functional magnetic particles associated with an electrode, which branches the application of functional magnetic nanoparticles out into the field of electrochemistry.[11] Magnetic functional nanoparticles have been easily prepared for biosensing, immunosensing, DNA sensing, ECL sensing, and fuel cells.[12−16] Therefore, iron oxide nanoparticles are of great interest for the study of magnetic properties and for practical applications. Nevertheless, the reactivity of iron oxide nanoparticles has been shown to greatly increase as the particle dimensions are reduced, and particles with relatively small sizes may undergo rapid degradation when they are directly exposed to certain environments.[17] Consequently, a suitable coating is essential to overcome such limitations. With the properties of stability, biocompatibility, and easy functionality, silica acts as an optimum alternative to encapsulate these magnetic nanoparticles.[18−20]

Recently, people are paying more attention to the preparation and application of dye-encapsulated silica nanoparticles.[21−25] On one hand, the encapsulation of fluorescent dye in nanoparticles often increases their photostability and emission quantum yield due to their isolation from possible quenchers such as molecular oxygen and water. On the other hand, the silica is relatively easy to functionalize and conjugate to bioactive molecules, which shows great potential in bioanalysis. As a whole, there are two methods to prepare the fluorescent dye-encapsulated silica nanoparticles: the microemulsion method and the Stöber method. Nanoparticles prepared by the reverse microemulsion method show good promise in size control and further miniaturization, but this technique requires the use of large amounts of surfactants and organic solvents, which means much effort to separate the nanoparticles from the large amount of surfactants.[26] Nevertheless, the Stöber method is simple and is carried out in an ethanol/water mixture, completely avoiding the use of potentially toxic organic solvents and surfactants. Furthermore, slight modification of the ammonia and water content in the reaction mixture results in monodispersed silica spheres of different diameters.[27] Among many dyes encapsulated, $Ru(bpy)_3^{2+}$ proves to be a suitable one due to its good stability and high quantum yield. Besides, its strong electrostatic interaction with silica makes its leaching negligible. Consequently, $Ru(bpy)_3^{2+}$-encapsulated silica nanoparticles are extensively applied in bioanalysis and biodetection.[28−29] And more recently, people began to be more aware of their application in electrochemiluminescence (ECL), as $Ru(bpy)_3^{2+}$ is a typical ECL reagent and a large quantity of $Ru(bpy)_3^{2+}$ molecules are three-dimensionally encapsulated inside each silica nanoparticle, which finally leads to the high ECL signal.[30−32]

Generally, a lot of work has been focused on fabricating bifunctional nanoarchitecture by combining the magnetic nanoparticles with the luminescent reagents.[33−36] Here, we synthesize a new kind of nanoarchitecture containing a magnetic Fe_3O_4 core and a luminescent $Ru(bpy)_3^{2+}$-encapsulated silica shell.

* Corresponding author. Fax: +86-431-85689-711. E-mail: dongsj@ns.ciac.jl.cn.

10.1021/jp0734427 CCC: $37.00
Published on Web 08/15/2007

These complex nanoparticles were characterized by transmission electron microscopy (TEM), vibrating sample magnetometer (VSM), and emission spectroscopy. Furthermore, unlike previous reports, we explored a new application of these bifunctional nanoparticles to fabricate an efficient ECL sensor. The sensitive and stable $Ru(bpy)_3^{2+}$ ECL sensor was based on the multilayer films of the as-prepared magnetic and luminescent nanoparticles stimulated by an external magnet. With such sensor, satisfying results were obtained with both $Ru(bpy)_3^{2+}$ typical coreactant TPA and practically significant polyamines.

2. Experimental Section

2.1. Reagents and Instruments. Tris(2,2′-bipyridyl) dichlororuthenium(II) hexahydrate ($Ru(bpy)_3Cl_2 \cdot 6H_2O$) and tripropylamine (TPA) were purchased from Aldrich and used without further treatment. The polyamines Spd and Spm were purchased from Sigma. Tetraethylorthosilicate (TEOS) was obtained from Beijing Yili Chemical Reagent Factory (Beijing, China). Ferric chloride, ferrous chloride, and ammonium hydroxide (25−28 wt %) were purchased from Beijing Chemical Reagent Factory (Beijing, China). All other chemicals were of analytical grade, and the aqueous solutions were prepared with doubly distilled water. Transmission electron microscopy (TEM) measurements were performed with a HITACHI H-8100 EM with an acceleration voltage of 200 kV. A drop of the core−shell nanoparticle aqueous solution was cast on a copper grid and allowed to dry. Magnetization of the iron oxide nanoparticles and bifunctional nanoparticles were measured by a vibrating sample magnetometer (VSM, LakeShore). Emission spectroscopy data were obtained from a LS 55 luminescence spectrometer (Perkin-Elmer, U.K.) at room temperature, and the excitation wavelength was selected at 460 nm. Lifetime was measured with PTI (Photo Technology International, (Canada). Cyclic voltammetric experiments were performed with a CH Instruments 832 voltammetric analyzer. The working electrode was a glassy carbon wafer coated with a multilayer film of magnetic and luminescent nanoparticles driven by an external magnet. A platinum wire was used as the counter electrode, and an Ag/AgCl (saturated KCl) as a reference electrode. The ECL signal produced in the electrolytic cell was detected and recorded by a flow injection chemiluminescence analyzer (IFFD, Xi'an Remax Electronic Science Tech. Co. Ltd. China), which was operated by a personal computer.

2.2. Preparation of Magnetic Iron Oxide Nanoparticles. The iron oxide nanoparticles were prepared according to Massart's method.[37] In a typical experiment, a mixed aqueous solution of ferric chloride (50 mL, 1 M) and ferrous chloride (10 mL, 2 M, in 2 M HCl) were added into ammonia solution (500 mL, 0.7 M) under vigorous stirring for 30 min at room temperature in a nitrogen atmosphere. The instantaneously formed black precipitate was separated by centrifugation and further washed with water at least three times. Then to a mixture of 3 mL of NH_4OH, 28.8 mL of H_2O, 27.5 mL of ethanol, and 6.22 mL of as-prepared iron oxide nanoparticle aqueous solution was added an ethanol solution of TEOS (1.5 mL of TEOS in 30 mL of EtOH) while the solution was vigorously stirred. The hydrolysis and condensation of TEOS onto the magnetic nanoparticles was completed in 2 h. Then the prepared nanoparticles were washed with ethanol and water several times, and finally they were dispersed in ethanol. Here the prepared silica between magnetic core and the fluorescent dye shell was to prevent emission quenching through core−dye interactions.

2.3. Preparation of Core−Shell Nanostructure. The luminescent shell was coated on the magnetic core with the Stöber method. First, 1.6 mL of TEOS, 10 mL of ethanol, and 500 μL of $Ru(bpy)_3^{2+}$ (1 mg/mL) solutions were premixed. Then 2 mL of as-prepared $Fe_3O_4@SiO_2$ was added into the mixture. Finally, 750 μL of ammonia solution was added, and the mixture was vigorously stirred for 3 h. Then the prepared nanoparticles were washed with ethanol and water. After evaporation of the solvent, the final core−shell nanostructure was obtained. The as-prepared $Fe_3O_4@SiO_2$ nanoparticles were used as nucleation sites, and the outer shell of luminescent $Ru(bpy)_3^{2+}$-encapsulated silica would grow onto them.

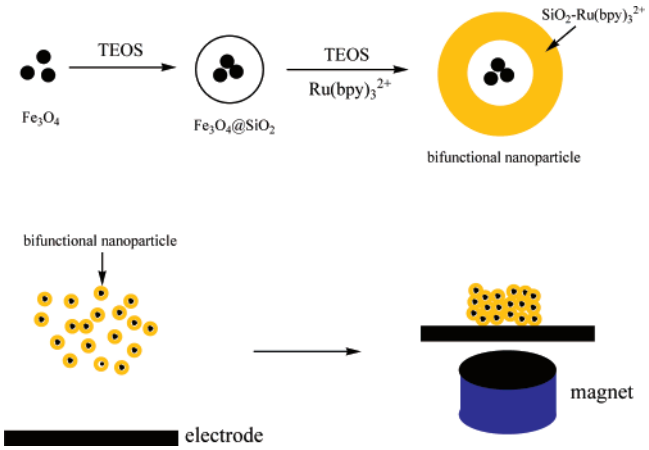

Figure 1. Scheme for the preparation of magnetic, luminescent nanoparticles, and fabrication of a bifunctional nanoparticle-modified electrode.

2.4. Preparation of Core−Shell Nanostructure Modified Electrode for ECL Detection. The glassy carbon wafer was polished before each experiment with 1 and 0.3 μm alumina powder, respectively, and sonicated thoroughly in acetone and doubly distilled water. Then an external magnet was positioned behind the wafer as demonstrated in Figure 1, and the electrode was placed in the bifunctional nanoparticle aqueous solution. The fabricated electrode attracted the magnetic luminescent nanoparticles, and the multilayer film of the bifunctional nanoparticles was formed within several minutes. The thickness of the multilayer film can be easily controlled by the variation of the amount of the magnetic luminescent nanoparticles introduced into the aqueous solution.

3. Results and Discussion

The Stöber method has been widely used for preparation of silica nanoparticles since it was first reported. It is simple,-convenient, and without surfactants and toxic organic solvents during the preparation process. Therefore, we use such method to prepare bifunctional nanoparticles. Figure 1 shows a schematic illustration of the preparation of core−shell nanoparticles with both magnetic and luminescent functionalities. First, silica-coated magnetic nanoparticles are synthesized. Since the iron oxide surface has a strong affinity for silica, no primer is required to promote the deposition and adhesion of silica.[38] The first silica layer covers the magnetic cores to isolate them from the outer-shell encapsulated dye molecules to prevent fluorescence quenching. Then the $Fe_3O_4@SiO_2$ nanoparticles act as seeds for the deposition of the $Ru(bpy)_3^{2+}$−silica shell. In this process, $Ru(bpy)_3^{2+}$ is immobilized in siloxane polymers during the growth of silica nanoparticles via the electrostatic interaction between positively charged $Ru(bpy)_3^{2+}$ and negatively charged silica. At last, the homogeneous $Ru(bpy)_3^{2+}$−silica is coated onto the $Fe_3O_4@SiO_2$ cores. Figure 2 shows TEM image of monodisperse and spherical bifunctional nanoparticles. In fact,

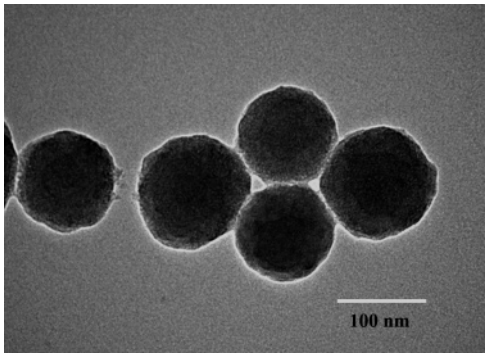

Figure 2. TEM of the prepared bifunctional nanoparticles.

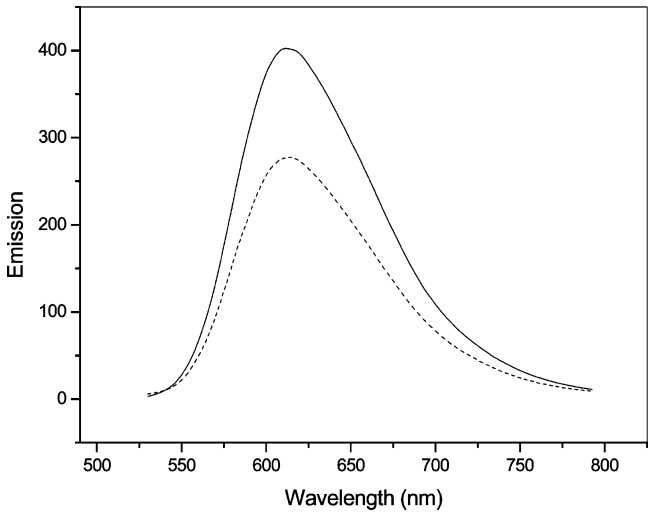

Figure 3. Emission spectra of $Ru(bpy)_3^{2+}$ aqueous solution (solid line) and $Ru(bpy)_3^{2+}$ encapsulated in bifunctional nanoparticles (dashed line) (excitation at 460 nm).

we have carried out a control experiment to synthesize the bifunctional nanoparticles without the first layer of silica. With such method, both fluorescent and ECL properties of the prepared nanoparticles were impacted severely. Therefore, the first layer of silica plays an important role in preventing luminescence quenching between iron oxide nanoparticles and luminescent $Ru(bpy)_3^{2+}$.

We compare the emission spectrum of the as-prepared nanoparticles with that of $Ru(bpy)_3^{2+}$ aqueous solution. The luminescent excited state of $Ru(bpy)_3^{2+}$ is assigned to the metal-to-ligand charge-transfer (MLCT) state. Judging from Figure 3, the bifunctional nanoparticles exhibit an emission peak at a position slightly red-shifted from that of the pristine $Ru(bpy)_3^{2+}$, which could be attributed to the interaction between $Ru(bpy)_3^{2+}$ and silica. Moreover, it is known that O_2 can promote fluorescence quenching because it deactivates the excited state of $Ru(bpy)_3^{2+}$.[28] However, the $Ru(bpy)_3^{2+}$ encapsulated in bifunctional nanoparticles exhibits a longer fluorescence lifetime compared with $Ru(bpy)_3^{2+}$ in aqueous solution. In aqueous solution, the $Ru(bpy)_3^{2+}$ fluorescence lifetime is about 400 ns, while the fluorescence lifetime of $Ru(bpy)_3^{2+}$ encapsulated in bifunctional nanoparticles is 805 ns. Consequently, it can be concluded that the silica matrix can protect immobilized $Ru(bpy)_3^{2+}$ from oxygen quenching and improve its photostability.

Magnetization curves, as shown in Figure 4, are measured on powder samples of iron oxide nanoparticles and bifunctional nanoparticles at room temperature. Both of them exhibit negligible coercivity and remanence, typical of superparamagnetic material. Their saturation magnetization is 68.8 and 9.7

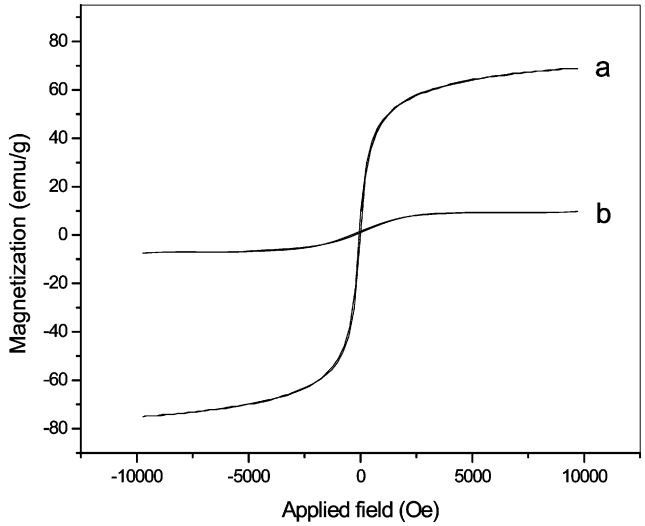

Figure 4. Magnetization curves of iron oxide nanoparticles (a) and bifunctional nanoparticles (b).

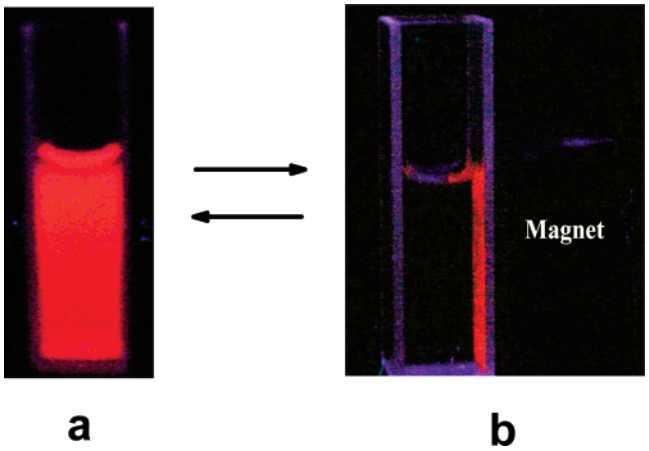

Figure 5. Photographic images of the magnetic luminescent nanoparticles under UV irradiation (a) without and (b) with an external magnetic field.

emu/g, respectively. Compared with the iron oxide, the relatively low saturation magnetization of bifunctional nanoparticles could be attributed to the thick shells of silica coated outside. Because of the magnetic iron oxide core, the composite particles can be directed to specific locations when manipulated by an external magnetic field, which, in this case, can be easily monitored through the intense luminescence of the bifunctional nanoparticles. Figure 5 illustrates the dispersion and separation process of these nanoparticles under UV irradiation. In the absence of an external magnet, the dispersion is homogeneous and bright orange. Once the magnet is placed beside the vial, the nanoparticles quickly move and accumulate near it within several minutes, with the bulk solution clear and transparent. With removal of the external magnet and vigorous stirring, the aggregations would be rapidly redispersed again.

With the unique architecture, the silica surface of the as-prepared nanoparticles remains available for versatile bioconjugation with various biomolecules. Therefore, the bifunctional nanoparticles could be extensively applied in imaging technology and bioanalysis, and a lot of research work has been explored. However, here we demonstrated a novel application of these bifunctional nanoparticles in an ECL field. Recently, extensive research has been devoted to the magnetic control of bioelectrochemical and electrochemical processes. An external magnet is used as a means to immobilize the electroactive

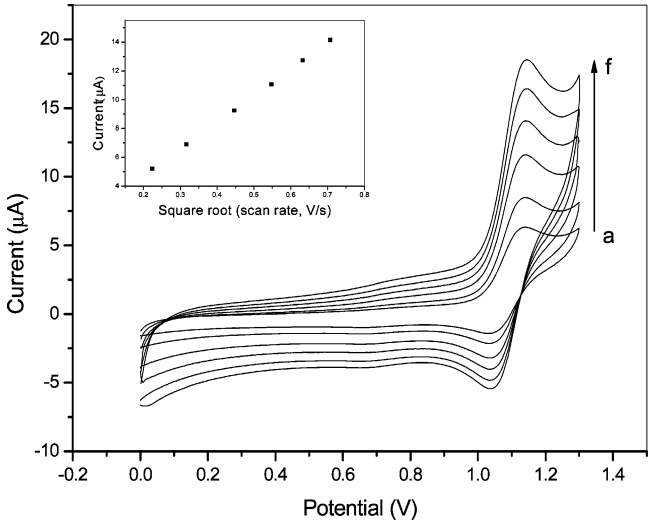

Figure 6. CVs of the ECL sensor at various scan rates in 0.1 M PBS (pH 7.5): (a) 50, (b) 100, (c) 200, (d) 300, (e) 400, and (f) 500 mV/s. (Inset) The relationship between the anodic peak current and the square root of the scan rate.

molecules onto the electrode surface and trigger the electrochemistry process. Such immobilization method is simple and effective; the key difficulty is how to link the electroactive molecules to the magnetic nanoparticles. The bifunctional nanoparticles we prepared just overcome this difficulty. The encapsulated iron oxide nanoparticles are superparamagnetic, while the $Ru(bpy)_3^{2+}$ immobilized in the outer shell still maintains its ECL property. Therefore, we use an external magnet to attract the as-prepared nanoparticles onto the electrode surface to form multilayer films, accordingly, a sensitive and stable ECL sensor is fabricated.

Cyclic voltammograms (CVs) of the bifunctional nanoparticle-modified electrode in 0.1 M PBS (pH 7.5) at different scan rates are shown in Figure 6, and a plot of oxidation peak current versus the square root of scan rate is also shown in the inset of Figure 6. The anodic peak current is proportional to the square root of the scan rate over the range of 50−500 mV/s, indicating that the immobilized $Ru(bpy)_3^{2+}$ undergoes a diffusion process. The ECL behavior of $Ru(bpy)_3^{2+}$ encapsulated in the bifunctional nanoparticle-modified electrode is studied with tripropylamine (TPA), since the $Ru(bpy)_3^{2+}$−TPA system has been fully investigated and gives a stronger ECL signal than other reductants.[39] Figure 7 shows ECL curves of the prepared electrode with and without 7.4×10^{-5} M TPA at a scan rate of 10 mV/s in 0.1 M PBS (pH 7.5). The ECL signal increases considerately once the TPA is added. The excellent ECL behavior is attributed to large amounts of $Ru(bpy)_3^{2+}$ immobilized on the electrode surface. With TPA as the probe, we evaluate the sensitivity and stability of the prepared ECL sensor. The ECL signal varies linearly with the concentration of TPA from 6.9×10^{-8} to 7.3×10^{-4} M (Figure 8) with a remarkable detection limit of 6.5 nM (S/N = 3). Compared with the effective $Ru(bpy)_3^{2+}$ preconcentration medium Nafion, the detection limit of the present ECL sensor is 2 orders of magnitude lower. The improved sensitivity could be attributed to the large amount of $Ru(bpy)_3^{2+}$ encapsulated in each bifunctional nanoparticle. The relative standard deviation of the ECL emission from the modified electrode under continuous potential scanning for 16 cycles in 0.1 M PBS (pH 7.5) containing 3.8×10^{-4} M TPA was 0.5%. After two-week storage of the as-prepared ECL sensor under the external magnet in the air, the ECL response could retain 85% of its initial value.

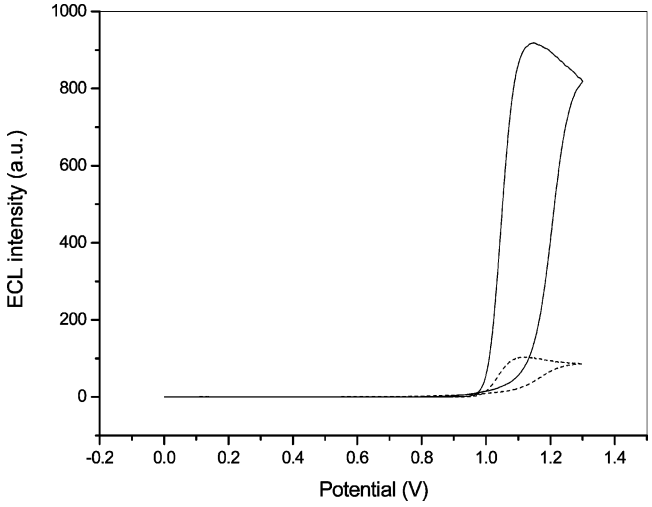

Figure 7. ECL curves of the prepared electrode with (solid line) and without (dashed line) 7.4×10^{-5} M TPA at a scan rate of 10 mV/s in 0.1 M PBS (pH 7.5).

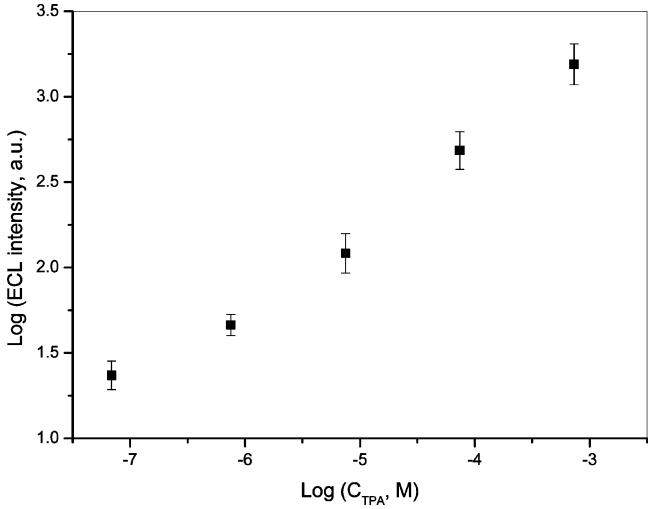

Figure 8. Calibration of TPA with the as-prepared ECL sensor in PBS (pH 7.5) at the scan rate of 100 mV/s.

The good stability of the ECL sensor may be attributed to the two different kinds of interactions: the electrostatic interaction between positively charged $Ru(bpy)_3^{2+}$ and negatively charged silica, and the magnetic interaction between bifunctional nanoparticles and the external magnet.

With high sensitivity, here we put the as-prepared ECL sensor to the practical application of detecting polyamines. The polyamines are constituents of eukaryotic and prokaryotic cells, fulfilling indispensable roles in human metabolism.[40] Moreover, some types of malignant cell proliferation are associated with increased cellular polyamine metabolism, and several investigators have suggested a possible role of polyamine determination in blood and urine samples as markers of the presence of malignancies.[41] The studies of polyamines are of great interest not only for their suitability as cancer markers, but also as an indicator of food quality and plant study.[42,43] However, since polyamines show neither UV absorption nor fluorescence, they cannot be determined with adequate sensitivity by spectrophotometric or fluorescence detection. Polyamines have to be derivatized or labeled before spectral detection.[44,45] However, the derivatization procedure makes the whole analytical process tedious and time-consuming. Polyamines are aliphatic amines containing different amine groups, that can be oxidized directly by $Ru(bpy)_3^{2+}$, so polyamines can be treated as analytes when

$Ru(bpy)_3^{2+}$-ECL detection is adopted without derivatization. Here, we chose polyamine spermidine (Spd) and spermine (Spm) as analytes. With our method, the linear ranges are 4×10^{-6} M to 5×10^{-3} M ($R = 0.988$) and 5.5×10^{-7} M to 10^{-4} M ($R = 0.999$) for Spd and Spm, respectively. And their detection limits are 8.4×10^{-7} M and 3.3×10^{-7} M (S/N = 3), respectively, which are 2 orders of magnitude lower than that reported for the ultraviolet method.[41] The reproducibility of the as-prepared ECL sensor was also examined. For three electrodes fabricated in the same manner, the relative standard deviation was 9.4% with an Spm concentration of 4.7×10^{-5} M.

4. Conclusions

The present work successfully prepared a new type of bifunctional nanoparticles containing a magnetic core and a $Ru(bpy)_3^{2+}$ encapsulated luminescent shell with the Stöber method. Highly luminescent $Ru(bpy)_3^{2+}$ acts as effective ECL reagent, while magnetic Fe_3O_4 nanoparticles allow external manipulation through a magnetic field. On the basis of their unique characteristics, we fabricated a novel ECL sensor. A good linear range from 6.9×10^{-8} M to 7.3×10^{-4} M with a remarkable detection limit of 6.5 nM (S/N = 3) to TPA was obtained, and the ECL relative standard deviation was only 0.5% during continuous potential scanning for 16 cycles. Moreover, we applied a prepared ECL sensor to polyamine detection, since these polyamines play a significant role but are difficult to detect directly. The detection limit with our method is 2 orders of magnitude lower than that reported for the ultraviolet method. Furthermore, because of the good biocompatibility and easy functionalization of silica, such bifunctional nanoparticles also have great potential in combination with ECL detection in bioanalysis.

Acknowledgment. This work was supported by the National Natural Science Foundation of China (No. 20427003, 20675076).

References and Notes

(1) Graf, C.; Dembski, S.; Hofmann, A.; Rühl, E. *Langmuir* **2006**, *22*, 5604.
(2) Doyle, P.; Bibette, J.; Bancaud, A.; Viovy, J. *Science* **2002**, *295*, 2237.
(3) Kouassi, G. K.; Irudayaraj, J. *Anal. Chem.* **2006**, *78*, 3234.
(4) Josephson, L.; Perea, J. M.; Weissleder, R. *Angew. Chem., Int. Ed.* **2001**, *40*, 3204.
(5) Ito, A.; Shinkai, M.; Honda, H.; Kobayashi, T. *Cancer Gene Ther.* **2001**, *8*, 649.
(6) (a) Shinkai, M. J. *Biosci. Bioeng.* **2002**, *94*, 606. (b) Jeong, U.; Teng, X.; Wang, Y.; Yang, H.; Xia, Y. *Adv. Funct. Mater.* **2007**, *19*, 33. (c) Gupta, A. K.; Gupta, M. *Biomaterials* **2005**, *26*, 3995.
(7) Safarikova, M.; Safarik, I. *Magn. Electr. Sep.* **2001**, *10*, 223.
(8) Pankhurst, Q. A.; Connolly, J.; Jones, S. K.; Dobson, J. *J. Phys. D: Appl. Phys.* **2003**, *36*, 167.
(9) Tartaj, P.; Morales, M. D. P.; Verdaguer, S. V.; Carreno, T. G.; Serna, C. J. *J. Phys. D: Appl. Phys.* **2003**, *36*, 182.
(10) Berry, C. C.; Curtis, A. S. G. *J. Phys. D: Appl. Phys.* **2003**, *36*, 198.
(11) Willner, I.; Katz, E. *Angew. Chem.. Int. Ed*. **2003**, *42*, 4576.
(12) Mavré, F.; Bontemps, M.; Ammar-Merah, S.; Marchal, D.; Limoges, B. *Anal. Chem.* **2007**, *79*, 187.
(13) Hirsch, R.; Katz, E.; Willner, I. *J. Am. Chem. Soc.* **2000**, *122*, 12053.
(14) Katz, E.; Ichia, L. S.; Willner, I. *Chem. Eur. J.* **2002**, *8*, 4138.
(15) Kim, D. J.; Lyu, Y. K.; Choi, H. N.; Min, I.; Lee, W. Y. *Chem. Commun*. **2005**, 2966.
(16) Wang, J.; Musameh, M.; Laocharoensuk, R.; Oni, J.; Gervasio, D. *Electrochem. Commun.* **2006**, *8*, 1106.
(17) Maceira, V. S.; Correa-Duarte, M. A.; Spasova, M.; Liz-Marzán, L. M.; Farle, M. *Adv. Funct. Mater*. **2006**, *16*, 509.
(18) Yi, D. K.; Lee, S. S.; Papaefthymiou, G. C.; Ying, J. Y. *Chem. Mater*. **2006**, *18*, 614.
(19) Yoon, T. J.; Kim, J. S.; Kim, B. G.; Yu, K. N.; Cho, M. H.; Lee, J. K. *Angew. Chem., Int. Ed.* **2005**, *44*, 1068.
(20) (a) Liz-Marzán, L. M.; Giersig, M.; Mulvaney, P. *Chem. Commun.* **1996**, 731. (b) Tartaj, P.; Serna, C. J. *J. Am. Chem. Soc.* **2003**, *125*, 15754. (c) Tartaj, P.; González-Carreño, T.; Serna, C. J. *Adv. Mater.* **2001**, *13*, 1620. (d) Ennas, G.; Musinu, A.; Piccaluga, G.; Zadda, D.; Gatteschi, D.; Sangregorio, C.; Stanger, J. L.; Concas, G.; Spano, G. *Chem. Mater*. **1998**, *10*, 495.
(21) Santra, S.; Yang, H.; Dutta, D.; Stanley, J. T.; Holloway, P. H.; Tan, W. H.; Moudgil, B. M.; Mericle, R. A. *Chem. Commun.* **2004**, 2810.
(22) Xian, Y. Z.; Liu, F.; Xian, Y.; Zhou, Y. Y.; Jin. L. T. *Electrochim. Acta* **2006**, *51*, 6527.
(23) Montalti, M.; Prodi, L.; Zaccheroni, N.; Battistini, G.; Marcuz, S.; Mancin, F.; Rampazzo, E.; Tonellato, U. *Langmuir* **2006**, *22*, 5877.
(24) Yao, H.; Li, N.; Xu, S.; Xu, J. Z.; Zhu, J. J.; Chen, H. Y. *Biosens. Bioelectron.* **2005**, *21*, 372.
(25) Bagwe, R. P.; Yang, C.; Hilliard, L. R.; Tan, W. H. *Langmuir* **2004**, *20*, 8336.
(26) Santra, S.; Zhang, P.; Wang, K.; Tapec, R.; Tan, W. H. *Anal. Chem.* **2001**, *73*, 4988.
(27) Stöber, W.; Fink, A.; Bohn, E. J. *Colloid Interface Sci*. **1968**, *26*, 62.
(28) Herr, J. K.; Smith, J. E.; Medley, C. D.; Shangguan, D.; Tan, W. *Anal. Chem.* **2006**, *78*, 2918.
(29) Smith, J. E.; Medley, C. D.; Tang, Z.; Shangguan, D.; Lofton, C.; Tan, W. *Anal. Chem.* **2007**, *79*, 3075.
(30) Zhang, L. H.; Dong, S. J. *Anal. Chem*. **2006**, *78*, 5119.
(31) Zhang, L. H.; Dong, S. J. *Electrochem. Commun*. **2006**, *8*, 1687.
(32) Chang, Z.; Zhou, J.; Zhao, K.; Zhu, N.; He, P. G.; Fang, Y. Z. *Electrochim. Acta* **2006**, *52*, 575.
(33) Hong, X.; Li, J.; Wang, M.; Xu, J.; Guo, W.; Li, J.; Bai, Y.; Li, T. *Chem. Mater*. **2004**, *16*, 4022.
(34) Kim, J.; Lee, J. E.; Lee, J.; Jang, Y.; Kim, S.; An, K.; Yu, J. H.; Hyeon, T. *Angew. Chem., Int. Ed.* **2006**, *45*, 4789.
(35) Lu, H.; Yi, G.; Zhao, S.; Chen, D.; Guo, L. H.; Cheng, J. *J. Mater. Chem*. **2004**, *14*, 1336.
(36) Ma, D.; Guan, J.; Normandin, F.; Dénommée, S.; Enright, G.; Veres, T.; Simard, B. *Chem. Mater*. **2006**, *18*, 1920.
(37) Massart, R. *IEEE Trans. Magn*. **1981**, *17*, 1247.
(38) Verónica, S.; Correa-Duarte, A. M.; Farle, M.; Quintela, A.; Sieradzki, K.; Diaz, R. *Chem. Mater*. **2006**, *18*, 2701; Lu, Y.; Yin, Y.; Mayers, B. T.; Xia, Y. *Nano Lett.* **2002**, *2*, 183.
(39) Noffsinger, J. B.; Danielson, N. D. *Anal. Chem.* **1987**, *59*, 865.
(40) Khuhawar, M. Y.; Qureshi, G. A. *J. Chromatogr., B* **2001**, *764*, 385−407.
(41) (a) Uehara, N.; Shirakawa, S.; Uchino, H.; Saeki, Y. *Cancer* **1980**, *45*, 108. (b) Russell, D. H. *Clin. Chem*. **1977**, *23*, 22.
(42) Kovács, A.; Simon-Sarkadi, L.; Ganzler, K. *J. Chromatogr., A* **1999**, *836*, 305.
(43) Bouchereau, A.; Aziz, A.; Larher, F.; Martin-Tanguy, *J. Plant. Sci.* **1999**, *140*, 103.
(44) Fu, S.; Zou, X.; Wang, X.; Liu, X. *J. Chromatogr., B* **1998**, *709*, 297.
(45) Taibi, G.; Schiavo, M. R.; Rindina, P. C.; Muratore, R.; Nicotra, C. M. A. *J. Chromatogr., A* **2001**, *921*, 323.